ELSEVIER

Contents lists available at ScienceDirect

Journal of Crystal Growth

journal homepage: www.elsevier.com/locate/jcrysgro



Molecular beam epitaxy and characterization of AlGaN nanowire ultraviolet light emitting diodes on Al coated Si (0 0 1) substrate



Yuanpeng Wu^a, Yongjie Wang^a, Kai Sun^b, Zetian Mi^{a,*}

- ^a Department of Electrical Engineering and Computer Science, University of Michigan, Ann Arbor, MI 48109, USA
- ^b Department of Materials Science and Engineering, University of Michigan, Ann Arbor, MI 48109, USA

ARTICLE INFO

Communicated by H. Asahi

Keywords:

A1. Nanostructures

- A1. Substrates
- A3. Molecular beam epitaxy
- B1. Nitrides
- B2. Semiconducting III-V materials
- B3. Light emitting diodes

ABSTRACT

We have demonstrated the epitaxial growth of AlGaN nanowires on Al coated Si $(0\,0\,1)$ substrate. The as-grown nanowires feature diameters of $> 200\,\mathrm{nm}$ and relatively uniform height distribution. AlGaN nanowires with emission wavelengths from 340 nm to 288 nm have been successfully achieved by varying Al/Ga beam equivalent pressure ratio and growth temperature. Detailed structural characterization suggests that AlGaN nanowires grown on Al template are free of dislocations. We have further demonstrated functional AlGaN nanowire deep ultraviolet (DUV) light emitting diodes, which exhibit a turn-on voltage of 7 V and a single peak EL emission at 288 nm. The realization of high quality AlGaN nanostructures on reflective Al template provides a promising approach for achieving high efficiency DUV light emitters.

1. Introduction

Deep ultraviolet (DUV) light emitting diodes (LEDs) and laser diodes (LDs) with wavelengths in the range of 200-350 nm are of great interest for a wide variety of applications including water and air purification, sterilization/disinfection, medical diagnostics, phototherapy, polymer curing, and sensing [1-6]. Among all the wide bandgap semiconductors, group III-nitrides (GaN, AlN, InN and their ternary and quaternary alloys) are deemed as the most suitable material family for the implementation of DUV LEDs and LDs [3,7-11]. Extensive efforts have been devoted to improving device performance in the past decades, and previously reported AlGaN based quantum well DUV LEDs often exhibit an EQE of less than 10% [12-15]. There are mainly three factors limiting the performance of DUV LEDs. First of all, typical threading dislocation density (TDD) of AlGaN heterostructures grown on sapphire is $\sim 10^9$ cm⁻², or higher, resulting in an internal quantum efficiency (IQE) of less than 50% [3,14,16,17]. Secondly, the large Mg activation energy in Al-rich AlGaN severely limits the available hole concentration, resulting in a low carrier injection efficiency [3,18]. Thirdly, light extraction efficiency (LEE) of the dominating transverse magnetic (TM) polarized emission in Al-rich AlGaN planar structure has been limited to 10% or less [17,19-21]. Very recently, through migration-enhanced metal organic chemical vapor deposition to reduce the threading dislocations (TDs) and by utilizing UV reflecting ohmic contacts and optimized chip encapsulation, an EQE of 20% at 20 mA

continuous wave (CW) injection for 275 nm DUV LEDs was achieved

AlGaN nanowires have emerged as a promising alternative to its planar counterparts in circumventing the above-mentioned challenges [23-26]. Dislocation-free nanowires can be achieved on lattice-mismatched substrate due to the efficient surface strain relaxation [27–30]. It has been shown that nanowires can be monolithically integrated on low cost substrate including Si [29,31,32], SiO₂ [33] and Ti [34,35]. Tran et al performed detailed investigation of MBE growth of Mg-doped nanowires and obtained hole concentration up to $\sim 6 \times 10^{17} \, \text{cm}^{-3}$, which is orders of magnitude higher compared with the reported values ($\sim 10^{12} \, \text{cm}^{-3}$) in Mg-doped AlN epilayers [26,36]. The significantly enhanced Mg incorporation was attributed to efficient hole hopping conduction in the Mg impurity band [36]. Liu et al showed that a maximum LEE > 90% can, in principle, be achieved for TM-polarized emission for AlGaN nanowire LEDs on reflective substrate [37]. To date, however, most of the reported nanowire based DUV devices are grown directly grown on Si substrate which is opaque to any UV emission and severely reduces the LEE.

A particular interest has been seen in growing nanowire structure on metals, and it has been envisioned that LEDs on metallic substrate have the advantages of excellent electrical and thermal conductivity [34,35,38–41]. Sarwar et al first reported growth of disks-in-nanowires on Mo coated Si (111) substrates [41]. Janjua et al demonstrated AlGaN nanowire based UV devices grown on a Ti coated n-type Si

E-mail address: ztmi@umich.edu (Z. Mi).

^{*} Corresponding author.

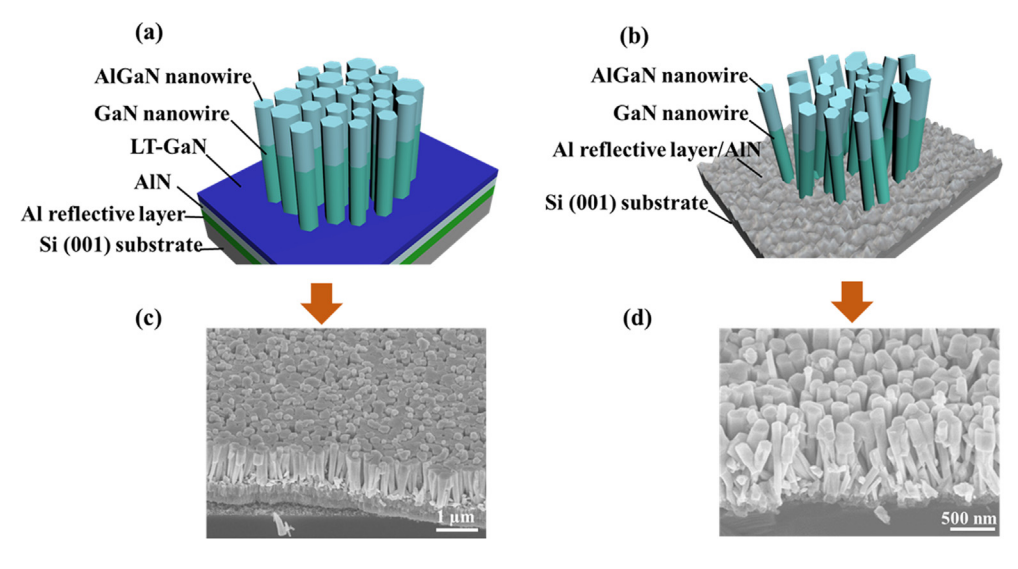


Fig. 1. MBE growth of GaN/AlGaN nanowires on Al coated Si (001) substrate. (a) Schematic of GaN/AlGaN nanowires grown on a LT-GaN on Al coated Si substrate. (b) Schematic of direct growth of GaN/AlGaN nanowires on Al coated Si substrate. (c) SEM image of GaN/AlGaN nanowires vertically integrated on Al coated Si with LT-GaN buffer layer. (d) SEM image of randomly oriented AlGaN nanowires grown directly on Al coated Si substrate. The SEM images were taken with a 45° tilting angle.

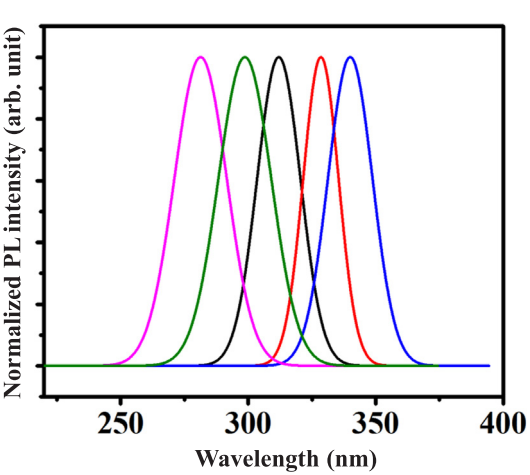


Fig. 2. Normalized PL spectra of samples grown under different Ga BEP and substrate temperatures with a nitrogen flow rate of 0.4 sccm. The blue, red and black curves correspond to samples grown with Ga BEP of 8×10^{-8} , 6×10^{-8} and 3.5×10^{-8} Torr, respectively at a substrate temperature of 780 °C. The green and magenta curves correspond to samples grown at a substrate temperature of 800 °C and 820 °C, respectively, with Ga BEP $\sim3.5\times10^{-8}$ Torr and Al BEP $\sim2\times10^{-8}$ Torr.

substrate. The device shows a UV emission wavelength of 337 nm and it's believed that the incorporation of Ti layer improved current injection and heat dissipation [39]. Prantie et al demonstrated that the incorporation of a thin metal layer could significantly reduce the junction temperature by 44 °C which further contributed to enhanced power and reliability of AlGaN devices [40].

Although Ti film can reflect $\sim 35\%$ light at 337 nm [39], the reflectivity plunges when moving to emission wavelengths shorter than 300 nm. Al has been widely adopted in UV reflectors with an over 85% reflectivity for emission wavelengths in the range of 250–300 nm. Moreover, Al has a thermal conductivity of 202 W/(m•K) while Ti has 22 W/(m•K) at room temperature, making it an ideal metal for enhancing the performance of DUV LEDs. However, due to its disadvantageous low melting temperature of 660 °C, to our best knowledge there have been no reports of AlGaN nanowires growth on Al film.

In this context, we have demonstrated epitaxial growth of AlGaN nanowires on Al coated Si substrate. A two-step growth method was utilized to realize high quality AlGaN nanowires vertically oriented on the substrate. The as-grown nanowires feature diameters of $> 200\,\mathrm{nm}$ and relatively uniform height distribution. AlGaN nanowires with emission wavelengths across nearly the entire UV-A and UV-B bands

have been successfully achieved by varying Al/Ga beam equivalent pressure (BEP) ratio and growth temperature. Detailed scanning transmission electron microscopy (STEM) characterization shows that the AlGaN nanowires were nearly free of TDs and stacking faults (SFs). The fabricated AlGaN nanowire LED devices have excellent rectification characteristics with a turn-on voltage of 7 V. A single peak electroluminescence (EL) emission at 288 nm was obtained. An EQE of $\sim 0.04\%$ was obtained at 20 A/cm² current injection which is at least one order of magnitude higher than the previous reports of AlGaN p-i-n nanowire based LEDs [6,30,42], except one most recent report wherein tunnel injection was utilized to enhance the device performance [43]. Significantly improved EQE is expected by optimizing the growth of AlGaN nanowire arrays directly on Al template and by eliminating light absorption through the Ni/Au p-contact metal on top of the AlGaN nanowire array.

2. Experimental procedure

In this work, AlGaN nanowire samples were grown using a Veeco Gen II MBE system equipped with a radio frequency nitrogen plasma source. All growths were performed on Al coated Si (0 0 1) substrate. The reflectivity of substrate was measured with a Woollam M-2000DI variable-angle spectroscopic ellipsometer in the wavelength range 193–900 nm. A 193 nm ArF excimer laser was used for photoluminescence (PL) excitation. PL spectra were acquired using a Horiba iHR550 spectrometer equipped with a UV-sensitive Synapse CCD matrix. The current-voltage (I-V) measurement was performed using a direct-current (DC) source meter (Keithley 2400). The electroluminescence (EL) spectra were collected using UV-enhanced optical fiber with numerical aperture (NA) of 0.22. The light output power was measured from the top of the nanowire DUV LEDs using a calibrated UV-enhanced Si photodetector (Newport 818-ST2-UV/DB).

3. Results and discussion

Prior loading into e-beam evaporator, the Si substrate was cleaned by buffered hydrofluoride solution to remove the surface oxide for all the samples studied. Then, Al film with a thickness of 300 nm was first deposited on the Si $(0\,0\,1)$ substrate at a rate of $2\,\text{Å/s}$ by e-beam evaporator at room temperature. Ellipsometry measurements show that the Al coated substrate has an over 85% reflectivity in the wavelength range of 250–400 nm at various incident angles. The Al template was cleaned using buffered hydrofluoride solution prior loading into the MBE chamber. After the Al coated Si substrate was loaded into intro chamber, it was thermally cleaned at 200 °C for 1 hr. Then the substrate

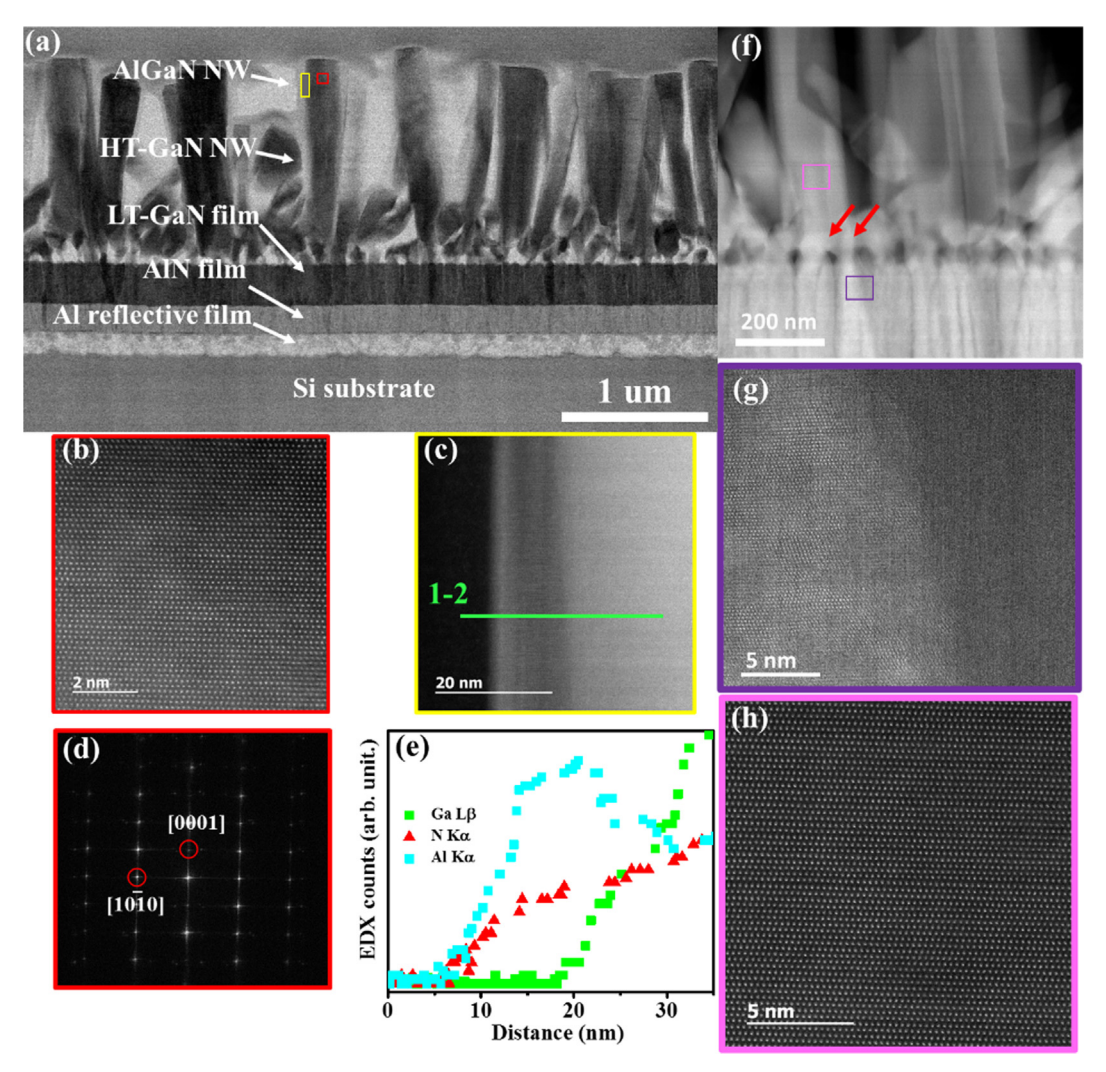


Fig. 3. (a) Low magnification cross-sectional STEM BF image of AlGaN/GaN nanowires on Al coated Si (001) substrate. (b, c) HAADF-STEM images of red and yellow boxed region of the AlGaN nanowire region. (d) FFT image of (b) shows that the AlGaN/GaN nanowire grows along the c-axis direction. (e) EDX line profile analysis along the lateral dimension of the AlGaN segment. (f) STEM-HAADF image of the interface between nanowires and LT-GaN layer. The red arrows point to the nucleation islands. (g) STEM-HAADF image of the purple-boxed region shows the out-of-plane crystallographic orientation of each column is aligned along the c-axis. (h) STEM-HAADF image of the magenta-boxed region in (f).

was transferred into buffer chamber and baked at 450 °C for 1 hr. A two-step growth method was adopted to realize vertically aligned AlGaN nanowires on Al template. GaN with a thickness of ~250 nm was firstly grown at a relatively low temperature (LT) of 600 °C as a buffer layer. During this process, an AlN layer was unintentionally formed underneath the GaN buffer. During the second step, while keeping the same Ga BEP of 1.5×10^{-7} Torr, nitrogen flow of 1 sccm, plasma forward power of 350 W and a relatively high temperature (HT) of 780 °C was utilized to induce the formation of GaN nanowires homoepitaxially on top of the LT-GaN layer. Fig. 1a shows the schematic of the AlGaN/GaN nanowire segments on such LT-GaN. The corresponding 45° tilt-view SEM image is shown in Fig. 1c. It can be observed that the obtained HT-GaN/AlGaN nanowire segments (sample A) are nearly vertically grown on the substrate with a relatively uniform height distribution. The density of the nanowire ensembles is $\sim 1 \times 10^9$ cm⁻² with diameters in the range of 200–350 nm, which are ~5-10 times larger than those grown on bare Si substrate under similar conditions [43]. The discrepancy can be attributed to the larger nucleation island size at the initial stage of HT-GaN nanowire growth as shown later. Direct growth of the nanowires on Al coated Si substrate without LT-GaN insertion was also investigated. As illustrated in Fig. 1b, d, the obtained nanowire array (sample B) features random outof-plane tilting to the substrate. It's worth mentioning that sample B is grown under identical conditions on the same substrate as sample A except that the LT-GaN buffer layer is not included. Moreover, the Al film thickness was reduced significantly to less than 20 nm while uniformity was also severely jeopardized, confirming the LT-GaN buffer layer is crucial in controlling the out-of-plane orientation of the nanowires. The random orientation could be attributed to the variation of nucleation sites on unstable Al film surface which undergoes severe adatom desorption at high growth temperature.

Subsequently, AlGaN nanowires were grown on the GaN nanowire template. The nitrogen flow rate was decreased to 0.4 sccm to enhance Al migration which was found to be essential to improve crystal quality [45]. A series of AlGaN samples were grown with the same Al BEP of $2.5\times10^{-8}\,\mathrm{Torr}$ while the Ga BEP was varied between 1×10^{-7} and $3.5\times10^{-8}\,\mathrm{Torr}$ at the same temperature of 780 °C in order to tune the emission wavelengths. As indicated by the blue, red and black curves in Fig. 2, the PL spectra exhibit a consistent blueshift with decreasing Ga BEP, and the full-width-at-half-maximum (FWHM) are $\sim20\,\mathrm{nm}.$ In order to achieve shorter wavelengths, the growth temperature for AlGaN nanowires was further raised from 780 °C to 820 °C to enhance Al adatom migration and Ga adatom desorption. AlGaN nanowire arrays with an emission wavelength of 288 nm, corresponding to Al

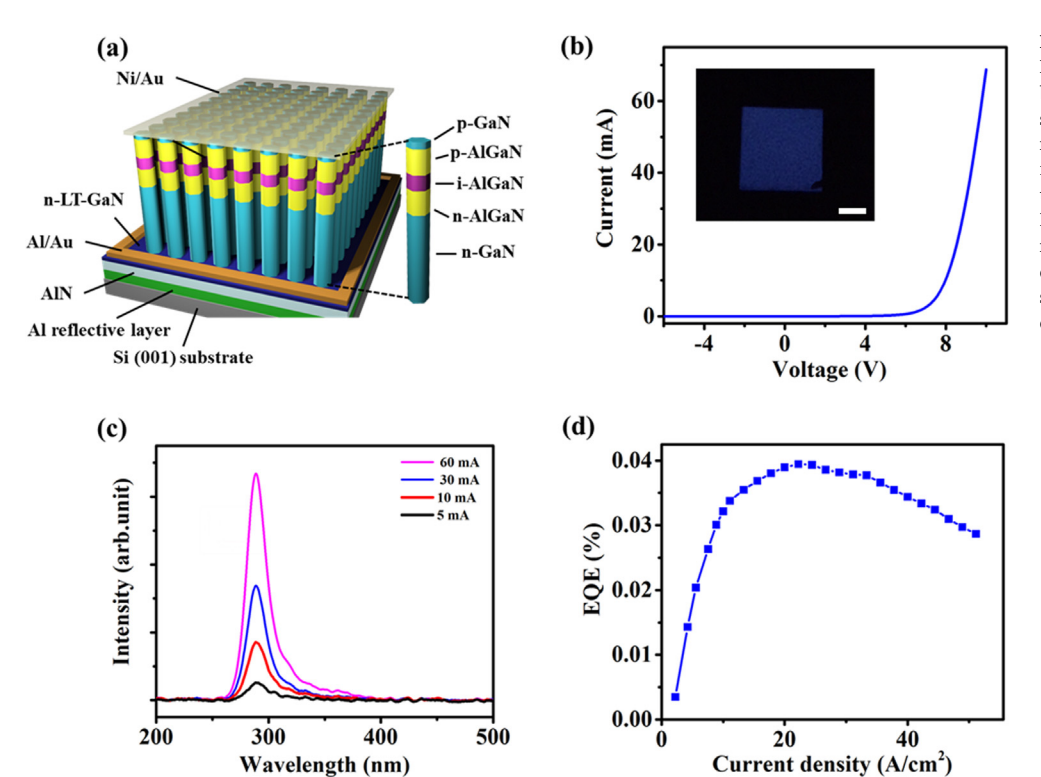


Fig. 4. Characteristics of AlGaN nanowire LEDs. (a) Schematic of AlGaN nanowire based DUV LED on Al coated Si (0 0 1) substrate. (b) I-V characteristics of AlGaN nanowire LEDs emitting at 288 nm, with the inset showing the optical image of LED under an injection current of 20 A/cm². Inset scale bar: 100 μm. (c) EL spectra measured from AlGaN nanowire LEDs with different injection currents. (d) The measured EQE vs. injection current of a device emitting at 288 nm.

composition of $\sim\!40\%$ in the UV-B region was obtained at a growth temperature of 820 $^{\circ}\text{C}.$

We have subsequently investigated structural properties of AlGaN nanowires grown on Al template. A cross-sectional specimen of the grown AlGaN/GaN nanowires with an emission wavelength of 288 nm was prepared by using an in-situ lift-out method performed using a FEI Helios 650 FIB/SEM dual beam system. Structural properties of the sample were studied using a JEOL JEM-3100R05 analytical electron microscope with double Cs-correctors operated at 300 keV. Fig. 3a shows the typical cross-sectional STEM bright field (BF) image of the GaN/AlGaN nanowires grown on Al coated Si substrate, wherein individual layers of the heterostructure can be clearly distinguished in the light of the varying image contrast. The GaN/AlGaN nanowires feature a large diameter of 200-350 nm and are nearly vertically aligned to the substrate. High resolution (HR) high-angle annular dark-field (HAADF) image of the red outlined region in Fig. 3b confirms the AlGaN segment is nearly free of TDs and SFs. Fast Fourier transform (FFT) (shown in Fig. 3d) of Fig. 3b confirms that the nanowire grows along c-axis with sidewalls being {1 1 0 0} planes. Fig. 3c shows the STEM-HAADF image of the yellow-boxed region in Fig. 3a, and the contrast variation along the lateral dimension indicates the presence of core-shell structure. Energy dispersive X-ray spectroscopy (EDX) line profile analysis was further performed along line 1-2. Shown in Fig. 3e, the Ga composition peak intensity increases toward the center of nanowire. In contrast, Al signals show a clear peak in the sidewall region and drop toward the center of the nanowire. This provides unambiguous evidence for the formation of a core-shell heterostructure, with the presence of an Alrich AlGaN shell surrounding the AlGaN core. Such a core-shell heterostructure has also been observed in previous studies [1,41,42,44]. The formation of Al-rich AlGaN shell provides effective carrier confinement in the nanowire LED active region and suppresses nonradiative surface recombination [22,46]. Fig. 3f further shows a STEM-HAADF image of the interface between the nanowires and LT-GaN layer, which features a columnar morphology. Nucleation islands with sizes of $\sim 75 \, \text{nm}$ were formed on top of the columns as pointed by the red arrows. These nucleation islands are significantly larger than their counterpart grown on Si substrate where a typical diameter of $\sim 10 \text{ nm}$

was reported [47,48], resulting in a large diameter of the subsequent GaN/AlGaN nanowire. SFs were observed in the LT-GaN buffer as shown in Fig. 3g, while the HT-GaN nanowires were nearly free of TDs and SFs (Fig. 3h).

The device schematic is shown in Fig. 4a, which consists of ~150 nm Al reflective layer on Si (001) substrate followed by ~250 nm Ge-doped LT-GaN layer. Ge-doped HT-GaN nanowire template was grown on top of the GaN buffer layer. Then n-AlGaN, i-AlGaN and p-AlGaN segments of 100, 60 nm and 100 nm were grown sequentially on top of the HT-GaN nanowire template. The Ge concentration of n-AlGaN is $\sim 5 \times 10^{19}$ cm⁻³, and the Mg concentration of p-AlGaN is $\sim 1 \times 10^{20} \, \text{cm}^{-3}$. On top of the p-AlGaN segments, 5 nm of p-GaN contact layer was grown with Mg concentration $\sim 5 \times 10^{19} \, \mathrm{cm}^{-3}$. The fabrication of AlGaN nanowire deep UV LEDs involves the use of standard lithography, plasma etching and contact metallization techniques. Ni (10 nm)/Au (10 nm) was deposited on top of the nanowire array using a tilted angle deposition to serve as p-metal contact. It's worthwhile mentioning that no filling materials were used to avoid the absorption of UV photons. Device mesa with various sizes was then patterned by photolithography and plasma etching using Cl₂/ BCl₃/Ar. Al(100 nm)/Au(50 nm) was deposited on Ge-doped LT-GaN layer to serve as n-metal contact. I-V characteristics of the AlGaN p-i-n structures were measured under CW biasing condition. The devices showed a typical turn-on voltage of 7 V. The device specific resistance estimated from the linear region of the forward I-V characteristics (between 8 and 10 V) was $\sim 35 \Omega$ for AlGaN nanowire UV LEDs, shown in Fig. 4b. The optical image of the device under 20 A/cm² injection current was shown in Fig. 4b inset. EL from a device with an areal size of 300 µm by 300 µm was measured under different injection current densities. It can be observed that the peak emission wavelength is 288 nm which matches very well with the PL measurement results. The peak position is invariant of the injection current, shown in Fig. 4c. The FWHM of the EL peak is ~17 nm. The measured EQE at room temperature under CW operation was shown in Fig. 4d. It can be seen that the EQE first increases with injection current and reaches a maximum value of ~0.04% at around 20 A/cm² before decreasing with further increasing current. It's worth noting that the obtained EQE of asfabricated devices is severely limited by the following factors. First, a large portion of the emitted light was absorbed by the Ni/Au p-contact layer atop AlGaN nanowires. Our previous finite-differential-time-domain (FDTD) simulation showed that Ni/Au of $\sim\!25\,\mathrm{nm}$ could result in a low LEE of $\sim\!0.4\%$ [1]. In order to avoid DUV light absorption by the absorptive p-metal, nanowire coalescence could be introduced so that metal contact can be deposited around the edge of the devices [43]. Secondly, the decreasing EQE with increasing current indicates the existence of electron overflow from the active region. Therefore, electron blocking layers with sufficient high barrier height are required to achieve a high carrier injection efficiency. Thirdly, the present GaN buffer absorbs UV emission shorter than 365 nm and an AlGaN buffer layer is required to achieve significantly enhanced EQE.

4. Conclusion

In conclusion, we have demonstrated epitaxial growth of AlGaN nanowire heterostructures on Al coated Si substrate. We have shown that the utilization of LT-GaN buffer layer can overcome the out-ofplane tilting issue and lead to the formation of nanowires vertically oriented to the substrate. The obtained nanowires feature uniform height distribution and diameters of > 200 nm. PL wavelengths tuning from 340 nm to 288 nm have been successfully achieved by varying Al/ Ga BEP ratio and growth temperature of AlGaN nanowires. Detailed structural characterizations suggest that the as-grown AlGaN nanowires are largely free of TDs and SFs. We have further fabricated functional AlGaN nanowire LEDs on Al coated Si(001) substrate which exhibit relatively good I-V characteristics. A single peak EL emission at 288 nm was obtained under different current injections. EQE of ~0.04% was obtained at 20 A/cm2 injection current. Further improved EQE is expected by removing the absorptive Ni/Au p-contact metal on top of the AlGaN nanowire array, reducing electron overflow by introducing electron blocking layers, and replacing GaN buffer with Al-rich AlGaN buffer layer.

Acknowledgements

The authors acknowledge the financial support of National Science Foundation (Grant DMR-1807984).

References

- [1] Z. Mi, S. Zhao, S.Y. Woo, M. Bugnet, M. Djavid, X. Liu, J. Kang, X. Kong, W. Ji, H. Guo, Z. Liu, G.A. Botton, J. Phys. D: Appl. Phys. 49 (2016) 364006.
- [2] K.P. Streubel, H. Hirayama, H. Jeon, L.-W. Tu, N. Linder, Proc. SPIE 7617 (2010) 76171G.
- [3] K. Ding, V. Avrutin, Ü. Özgür, H. Morkoç, Crystals 7 (2017) 300.
- [4] Y. Wu, T. Hasan, X. Li, P. Xu, Y. Wang, X. Shen, X. Liu, Q. Yang, Appl. Phys. Lett. 106 (2015) 051108.
- [5] Q. Yang, W. Wang, S. Xu, Z.L. Wang, Nano Lett. 11 (2011) 4012.
- [6] T.F. Kent, S.D. Carnevale, A.T. Sarwar, P.J. Phillips, R.F. Klie, R.C. Myers, Nanotechnology 25 (2014) 455201.
- [7] D. Li, K. Jiang, X. Sun, C. Guo, Adv. Opt. Photonics 10 (2018) 43.
- [8] A.T. Sarwar, B.J. May, M.F. Chisholm, G.J. Duscher, R.C. Myers, Nanoscale 8 (2016) 8024.
- [9] Y. Aoki, M. Kuwabara, Y. Yamashita, Y. Takagi, A. Sugiyama, H. Yoshida, Appl. Phys. Lett. 107 (2015) 151103.

- [10] H. Yoshida, Y. Yamashita, M. Kuwabara, H. Kan, Appl. Phys. Lett. 93 (2008) 241106.
- [11] K.H. Li, X. Liu, Q. Wang, S. Zhao, Z. Mi, Nat. Nanotechnol. 10 (2015) 140.
- [12] S.-I. Inoue, N. Tamari, M. Taniguchi, Appl. Phys. Lett. 110 (2017) 141106.
- [13] M. Jo, N. Maeda, H. Hirayama, Appl. Phys. Express 9 (2016) 012102.
- [14] M. Ichikawa, A. Fujioka, T. Kosugi, S. Endo, H. Sagawa, H. Tamaki, T. Mukai, M. Uomoto, T. Shimatsu, Appl. Phys. Express 9 (2016) 072101.
- [15] S.-I. Inoue, T. Naoki, T. Kinoshita, T. Obata, H. Yanagi, Appl. Phys. Lett. 106 (2015) 131104.
- [16] J.R. Grandusky, J. Chen, S.R. Gibb, M.C. Mendrick, C.G. Moe, L. Rodak, G.A. Garrett, M. Wraback, L.J. Schowalter, Appl. Phys. Express 6 (2013) 032101.
- [17] P. Dong, J. Yan, J. Wang, Y. Zhang, C. Geng, T. Wei, P. Cong, Y. Zhang, J. Zeng, Y. Tian, L. Sun, Q. Yan, J. Li, S. Fan, Z. Qin, Appl. Phys. Lett. 102 (2013) 241113.
- [18] H. Hirayama, N. Maeda, S. Fujikawa, S. Toyoda, N. Kamata, Jpn. J. Appl. Phys. 53 (2014) 100209.
- [19] S. Zhao, M. Djavid, Z. Mi, Nano Lett. 15 (2015) 7006.
- [20] J. Shakya, K. Knabe, K.H. Kim, J. Li, J.Y. Lin, H.X. Jiang, Appl. Phys. Lett. 86 (2005) 091107.
- [21] T. Kolbe, A. Knauer, C. Chua, Z. Yang, S. Einfeldt, P. Vogt, N.M. Johnson, M. Weyers, M. Kneissl, Appl. Phys. Lett. 97 (2010) 171105.
- [22] T. Takano, T. Mino, J. Sakai, N. Noguchi, K. Tsubaki, H. Hirayama, Appl. Phys. Express 10 (2017) 031002.
- [23] S. Zhao, H.P.T. Nguyen, M.G. Kibria, Z. Mi, Prog. Quant. Electron. 44 (2015) 14.
- [24] M. Djavid, Z. Mi, Appl. Phys. Lett. 108 (2016) 051102.
- [25] S. Zhao, S.Y. Woo, M. Bugnet, X. Liu, J. Kang, G.A. Botton, Z. Mi, Nano Lett. 15 (2015) 7801.
- [26] S. Zhao, A.T. Connie, M.H. Dastjerdi, X.H. Kong, Q. Wang, M. Djavid, S. Sadaf, X.D. Liu, I. Shih, H. Guo, Z. Mi, Sci. Rep. 5 (2015) 8332.
- [27] K. Hestroffer, R. Mata, D. Camacho, C. Leclere, G. Tourbot, Y.M. Niquet, A. Cros, C. Bougerol, H. Renevier, B. Daudin, Nanotechnology 21 (2010) 415702.
- [28] Q. Wang, A.T. Connie, H.P. Nguyen, M.G. Kibria, S. Zhao, S. Sharif, I. Shih, Z. Mi, Nanotechnology 24 (2013) 345201.
- [29] Q. Wang, H.P.T. Nguyen, K. Cui, Z. Mi, Appl. Phys. Lett. 101 (2012) 043115.
- [30] A.T.M.G. Sarwar, B.J. May, J.I. Deitz, T.J. Grassman, D.W. McComb, R.C. Myers, Appl. Phys. Lett. 107 (2015) 101103.
- [31] S. Zhao, X. Liu, S.Y. Woo, J. Kang, G.A. Botton, Z. Mi, Appl. Phys. Lett. 107 (2015) 043101.
- [32] A. Pierret, C. Bougerol, S. Murcia-Mascaros, A. Cros, H. Renevier, B. Gayral, B. Daudin, Nanotechnology 24 (2013) 115704.
- [33] Z. Gu, M.P. Paranthaman, J. Xu, Z.W. Pan, ACS Nano 3 (2009) 273.
- [34] B.J. May, A.T.M.G. Sarwar, R.C. Myers, Appl. Phys. Lett. 108 (2016) 141103.
- [35] C. Zhao, T.K. Ng, N. Wei, A. Prabaswara, M.S. Alias, B. Janjua, C. Shen, B.S. Ooi, Nano Lett. 16 (2016) 1056.
- [36] N.H. Tran, B.H. Le, S. Zhao, Z. Mi, Appl. Phys. Lett. 110 (2017) 032102.
- [37] X. Liu, K. Mashooq, T. Szkopek, Z. Mi, IEEE Photonics J. 10 (2018) 1.
- [38] M. Wolz, C. Hauswald, T. Flissikowski, T. Gotschke, S. Fernandez-Garrido, O. Brandt, H.T. Grahn, L. Geelhaar, H. Riechert, Nano Lett. 15 (2015) 3743.
- [39] B. Janjua, H. Sun, C. Zhao, D.H. Anjum, D. Priante, A.A. Alhamoud, F. Wu, X. Li, A.M. Albadri, A.Y. Alyamani, M.M. El-Desouki, T.K. Ng, B.S. Ooi, Opt. Express 25 (2017) 1381.
- [40] D. Priante, R.T. Elafandy, A. Prabaswara, B. Janjua, C. Zhao, M.S. Alias, M. Tangi, Y. Alaskar, A.M. Albadri, A.Y. Alyamani, T.K. Ng, B.S. Ooi, J. Appl. Phys. 124 (2018) 015702
- [41] A.T.M.G. Sarwar, S. Carnevale, F. Yang, T. Kent, J. Jamison, D. McComb, R. Myers, Small 11 (2016) 5402.
- [42] S. Zhao, S.M. Sadaf, S. Vanka, Y. Wang, R. Rashid, Z. Mi, Appl. Phys. Lett. 109 (2016) 201106.
- [43] S.M. Sadaf, S. Zhao, Y. Wu, Y.H. Ra, X. Liu, S. Vanka, Z. Mi, Nano Lett. 17 (2017) 1212.
- [44] Y. Wu, Y. Wang, K. Sun, A. Aiello, P. Bhattacharya, Z. Mi, J. Cryst. Growth 498 (2018) 109.
- [45] S. Zhao, S.Y. Woo, S.M. Sadaf, Y. Wu, A. Pofelski, D.A. Laleyan, R.T. Rashid, Y. Wang, G.A. Botton, Z. Mi, Molecular beam epitaxy growth of Al-rich AlGaN nanowires for deep ultraviolet optoelectronics, APL Mater. 4 (2016) 086115.
- [46] B.T. Tran, H. Hirayama, Sci. Rep. 7 (2017) 12176.
- [47] V. Consonni, M. Knelangen, A. Trampert, L. Geelhaar, H. Riechert, Appl. Phys. Lett. 98 (2011) 071913.
- [48] J. Ristić, E. Calleja, S. Fernández-Garrido, L. Cerutti, A. Trampert, U. Jahn, K.H. Ploog, J. Cryst. Growth 310 (2008) 4035.